Available online at www.sciencedirect.com
ScienceDirect
Journal of the European Ceramic Society 28 (2008) 591–597
www.elsevier.com/locate/jeurceramsoc

Deposition of $PbTiO_3$ films on Pt/Si substrates using pulsed laser deposition

Mikael A. Khan *, Timothy P. Comyn, Andrew J. Bell

Institute for Materials Research, University of Leeds, Leeds LS2 9JT, UK

Received 17 March 2007; received in revised form 18 July 2007; accepted 20 July 2007
Available online 22 October 2007

Abstract

Lead titanate ($PbTiO_3$) thin films were prepared on platinised silicon substrates by pulsed laser deposition. A predominantly (1 1 1) oriented perovskite phase was obtained at a substrate temperature of 530 °C. Deposition at higher substrate temperatures resulted in the formation of a lead deficient pyrochlore phase $PbTi_3O_7$. The (1 1 1) orientation was slightly enhanced with an increase in the oxygen deposition pressure from 100 mTorr to 150 mTorr. A similar effect was observed with an increase in the post-deposition annealing temperature from 400 °C to 600 °C. *P–E* loops with remanent polarization (P_r) as high as 40 μC/cm^2 and coercive field E_c = 105 kV/cm were obtained under an electric field of an amplitude of 270 kV/cm at 50 kHz. Impedance spectroscopy and leakage current behaviour of the films are also reported.

Keywords: Films; Electron microscopy; Ferroelectric properties; Perovskites; Pulsed laser deposition (PLD); $PbTiO_3$

1. Introduction

$PbTiO_3$ was first reported as a ferroelectric by Shirane et al. in 1950,[1] and was later employed in a solid solution with $PbZrO_3$ to form PZT (lead zirconate titanate) which is perhaps the single most significant piezoelectric material to date. The significance of using pure lead titanate for various device applications lies in the fact that it exhibits a high Curie temperature of 490 °C. At this temperature the material undergoes a first order transition from a *Pm*3*m* cubic perovskite structure to a *P*4*mm* tetragonal perovskite. At room temperature, it exhibits a lattice parameter of $c = 4.150$ Å and $a = 3.904$ Å,[2] thus giving a *c*/*a* as high as 1.063.

Recent advances in microelectronics and nanotechnology have prompted the requirement for ferroelectrics to be deposited in thin film form for a new generation of small and compact devices e.g. micro-actuators, micro-sensors and non-volatile memory applications. Extensive research on ferroelectric thin films has thus ensued, with researchers employing a number of thin film deposition techniques such as radio frequency magnetron sputtering,[3] chemical vapour deposition (CVD),[4] electron beam evaporation,[5] sol–gel[6] and more recently, pulsed laser deposition (PLD).[7]

Given its position as an archetypical ferroelectric with a comparatively large polarization it is surprising to find that there are very few accounts of the deposition of unmodified $PbTiO_3$ by PLD and even fewer concerning deposition on the most commercially relevant substrate, Pt/Si. Perhaps work of this nature has been limited by the difficulties in preparing ceramic targets, as the 6% spontaneous strain in conventionally prepared, pure $PbTiO_3$ results in disintegration of the body on cooling through the Curie temperature. Perhaps for this reason there are a larger number of reports on doped $PbTiO_3$ (e.g. La:$PbTiO_3$),[8–12] in which the spontaneous strain is much reduced. The difficulty of the spontaneous strain is avoided by the use of targetless preparation techniques such as solution deposition.[8,13–15]

The range of substrates upon which pure $PbTiO_3$ has been deposited is rather wide. Kang reported the growth of *c*-axis oriented $PbTiO_3$ films on single crystal $SrTiO_3$ and MgO substrates at temperatures ranging from 550 °C to 700 °C. Other authors have also reported the growth of lead titanate thin films on MgO substrates.[16–19] Deveirman presented TEM and XRD characterization of lead titanate thin films grown by PLD on $LaAlO_3$, $SrTiO_3$, MgO, and $MgAl_2O_4$. Wu prepared lead titanate thin films on Si substrates employing CeO_2 and Y_2O_3 buffer layers[20,21] while Purandare prepared oriented Si

* Corresponding author.
E-mail address: sms3mak@leeds.ac.uk (M.A. Khan).

0955-2219/$ – see front matter © 2007 Elsevier Ltd. All rights reserved.
doi:10.1016/j.jeurceramsoc.2007.07.023

substituted lead titanate thin films by pulsed laser deposition on Si(1 0 0) substrates.[22] However, the use of these substrates limits any property evaluation in the context of device integration on silicon.

Despite problems with significant leakage[23] pure lead titanate can be considered as a model system for tetragonal symmetry ferroelectric thin films and is therefore of significant interest. Given the lack of data relating to films produced by PLD, the current study was undertaken. Hence, this report presents a comprehensive analysis of the preparation of sintered targets and high quality film preparation using pulsed laser deposition. The report includes characterization of structure using X-ray diffraction (XRD), texture analysis, electron microscopy, analysis of the electrical properties including polarization-field response, impedance spectroscopy and the d.c. leakage behaviour.

2. Experimental

A pulsed laser system was employed for the deposition of $PbTiO_3$ thin films. The substrates were 10 mm × 10 mm × 0.5 mm oxidised Si(1 0 0), coated with Pt(1 1 1) and a 5 nm intermediate Ti wetting layer. The substrates were ultrasonically cleaned for 5 min each in Volasil 244 (octamethylcyclotetrasiloxane), acetone and isopropanol, respectively, followed by drying with nitrogen. The PLD system as shown in Fig. 1, is probably the simplest among all thin film growth techniques. The system comprises a vacuum chamber housing a target and substrate holder. A substrate heater is positioned immediately above the substrate holder. A set of lenses and mirrors is used to focus the laser beam over the target surface. A high power pulsed laser strikes the target at an angle of 45°, thus generating a plasma plume normal to the surface of the target which then transfers the target composition to a heated substrate. During the ablation process the target is simultaneously rotated and toggled to ensure uniform ablation and evaporation of the target surface. The decoupling of the evaporation power source and the vacuum hardware allow the system to be used without the constraints of internally powered evaporation sources. Film growth can be carried out in the presence of reactive gases which enhance the experimental possibilities. For our experiments a KrF 248 nm laser with a pulse width of 15×10^{-9} s was employed.

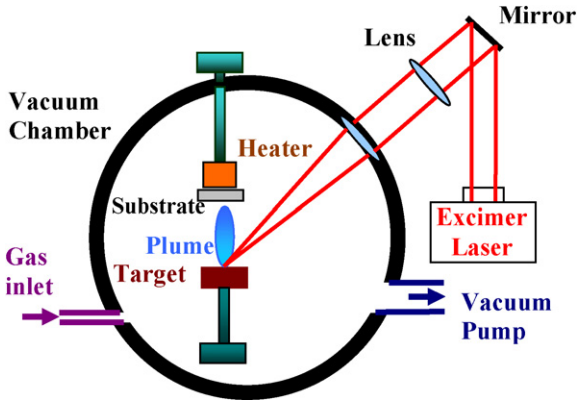

Fig. 1. Schematic of the PLD system.

Table 1
Deposition parameters

Laser fluence	8 J cm^{-2}
Frequency	5 Hz
Substrate temperature	530 °C
Deposition pressure	100–150 mTorr
Target–substrate distance	4 cm

Lead titanate targets were prepared by calcining stoichiometric ratios of attrition milled PbO (>99% purity, Aldrich Germany) and TiO_2 (>99% purity, Aldrich Germany) powders at 800 °C for 1 h. The calcined powders were then isostatically pressed at 200 MPa. Sintering of the compact was carried out at 900 °C for 15 min, followed by a slow cool below 530 °C to room temperature at 10 °C/h.

The PLD chamber was initially pumped down to 0.01 mTorr. The deposition parameters are shown in Table 1. After deposition the films were annealed at temperatures ranging from 400 °C to 600 °C under oxygen ambient of 3.8×10^5 mTorr. The films were annealed for a duration of 1 h. The annealing time has also been reported to affect the film crystallinity, which decreases considerably as the annealing time is increased beyond an hour.[24] The crystal structure of the films was determined by X-ray diffraction (Model X'pert PRO MPD, PANalytical, Almelo, The Netherlands) using Bragg–Brentano geometry. Scanning electron microscopy (SEM, Model 1530 FEGSEM, LEO electron microscopy group, Oberkochen, Germany) was performed to examine the surface morphology and film cross-section. The chemical composition of the films was determined by energy dispersive X-ray micro-analysis (EDX). Dielectric measurements were performed employing an impedance analyser (Agilent Precision Impedance Analyzer 4294A, Agilent Technologies, Palo Alto, U.S.A.) at room temperature. Leakage currents were measured using a programmable electrometer (Keithley 617, Keithley Instruments, Cleveland, U.S.A.). Impedance spectroscopy was performed using a Model 1296 Solartron dielectric interface connected to a Solartron impedance/gain-phase analyzer (Model 1260, Solartron Analytical, Farnborough, U.K.).

3. Results & discussion

3.1. Structural characterization

Fig. 2 shows the X-ray diffraction (XRD) pattern of the $PbTiO_3$ target. Profile fitting and peak fitting indicated a tetragonal crystal system with space group *P*4*mm* and lattice parameters of $c = 4.14$ Å (±0.001 Å) and $a = 3.896$ Å (±0.001 Å), resulting in $c/a = 1.0624$.

Films deposited at a substrate temperature greater than 585 °C indicated the presence of a pyrochlore $PbTi_3O_7$, which became a dominant phase at a substrate temperature of 640 °C. Chen et al.[25] have also reported the formation of this pyrochlore phase at temperatures above 570 °C for sol–gel films; and have related the pyrochlore formation to Pb loss. Fig. 3 is an XRD pattern

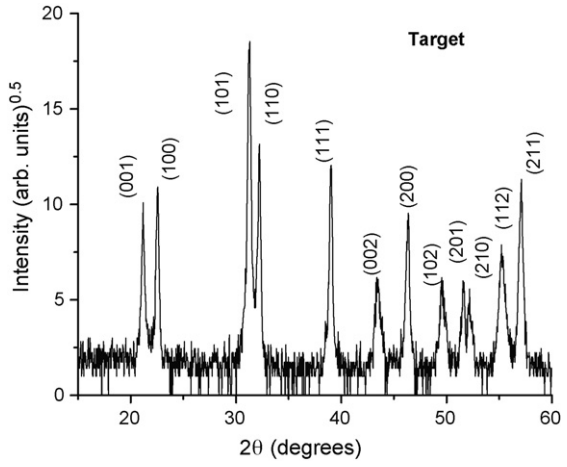

Fig. 2. XRD pattern of $PbTiO_3$ target.

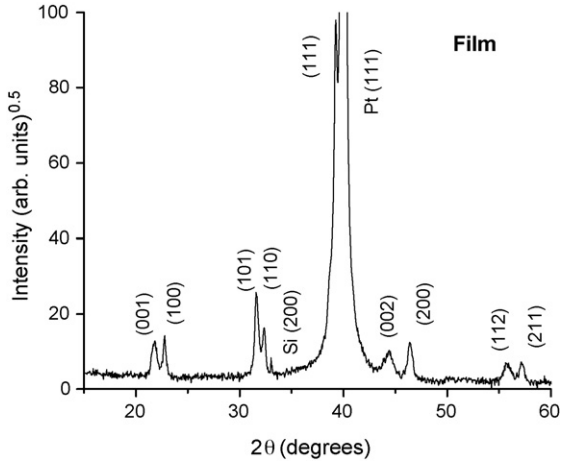

Fig. 3. XRD pattern of $PbTiO_3$ film deposited at 100 mTorr and 530 °C, followed by 600 °C anneal.

of a film deposited at a substrate temperature of 530 °C and indicates the presence of only the $PbTiO_3$ perovskite phase. The *d*-spacings after peak fitting are shown in Table 2. The out of plane *c* and *a* parameters show a 1.5% decrease and 0.5% increase, respectively when compared to the single crystal values. These differences are consistent with the thermal expansion mismatch between silicon and the *a*- and *c*-axis of $PbTiO_3$. Lee et al. have also reported a similar reduction in the tetragonality of films as compared to the bulk target, in compositionally modified lead titanate thin films.[9]

The degree of preferred orientation in a film can be represented by a definition proposed by Lotgering[26] which is as follows:

$$f(m\,n\,p) = \frac{I(m\,n\,p)}{\sum I(h\,k\,l)} \quad (1)$$

where $f(m\,n\,p)$ is the degree of preferred orientation, $I(m\,n\,p)$ is the intensity of the reflection. Table 3 compares the degree of preferred orientation in films formed at varying oxygen deposition pressure and post-deposition annealing temperature. Fig. 4 is a phi scan taken about the (1 0 0), (1 1 0) and (1 1 1) peaks, respectively. The results indicate a fibre texture in the film structure with preferential orientation along the [1 1 1] direction. High intensity poles were observed at 54° and 36° (ψ) for phi scans taken about the (1 0 0) and (1 1 0) planes, respectively, which are close to the interplanar angles for (1 1 1) planes to the (1 0 0) and (1 1 0) planes, respectively, for a cubic crystal system i.e. 54.7° and 35.3°. In the case of the phi scan obtained from the (1 1 1) planes, a very high intensity pole at 0° (ψ) as well as a pole at 70° (ψ) was observed. The pole at 70° (ψ) is commensurate with the interplanar angle for (1 −1 1) planes, which for a cubic system is 70.5°. Hence, all the films exhibit a preferred (1 1 1) orientation.

It can be seen that the higher post-deposition annealing temperature enhances the preferred orientation along the [1 1 1] direction. Also the percentage decrease in orientation along the [*h* 0 0] is higher as compared to that along the [0 0 l] direction. The increase in the deposition pressure also results in a corresponding increase in the orientation along the [1 1 1] direction. It is believed that the lower deposition pressure of 100 mTorr leads to an increase in the flux of target material on the substrate surface. This increases the nucleation and growth rate of grains on the substrate surface which would quickly impinge on one another resulting in the reduced degree of preferred orientation as compared to films deposited at 150 mTorr.

SEM images of films deposited at 150 mTorr are shown in Fig. 5. We can observe an increase in the average grain size of the film (from ∼170 nm to 250 nm) with an increase in the post-deposition annealing temperature. The films annealed at 600 °C appear more dense and we can see the presence of grain coalescence in Fig. 5b (indicated by arrows). A cross-sectional image of a fractured surface is shown in Fig. 6, with the films exhibiting an average thickness of 530 nm. We can observe well defined columnar grain growth extending through the entire film thickness with rounded tops. Previous reports suggest that the sub-grain structure develops, whilst preferred orientation develops through the sequential growth of coherent grains on top of one another.[11]

3.2. Electrical properties

Gold top electrodes of 0.3 mm diameter were sputter deposited on the films. The platinum coating was used as a bottom electrode. Fig. 7 shows the permittivity and dielectric loss of the film deposited under 150 mTorr of oxygen and annealed at 600 °C as a function of frequency. This film exhibited the highest permittivity ($\varepsilon' \approx 300$ at 100 kHz) compared to films prepared under other conditions. The rapidly increasing value of imaginary part with increasing frequency suggests some form of

Table 2
d-spacings

Planes	$d_{h,k,l=1}$	$d_{h,k,l=2}$	$d_{h,k=1,l=2}$	$d_{h=2,k,l=1}$
(0 0 *l*)	4.09240	2.04295		
(*h* 0 0)	3.91890	1.95704		
(*h* 0 *l*)	2.83330	1.41730		
(*h k* 0)	2.77155			
(*h k l*)	2.29855	1.14843	1.64860	1.61333

Table 3
Degree of preferred orientation

Films	Annealing temp. (°C)	f(0 0 1) (%)	f(1 0 0) (%)	f(1 0 1) (%)	f(1 1 0) (%)	f(1 1 1) (%)
100 mTorr	400	3.6	5.8	12.5	5	66.3
	600	3.3	4.5	5.7	1.9	78.9
150 mTorr	400	2.5	4.7	9.5	3.6	75.4
	600	1.8	2.2	8.0	3.0	82.2

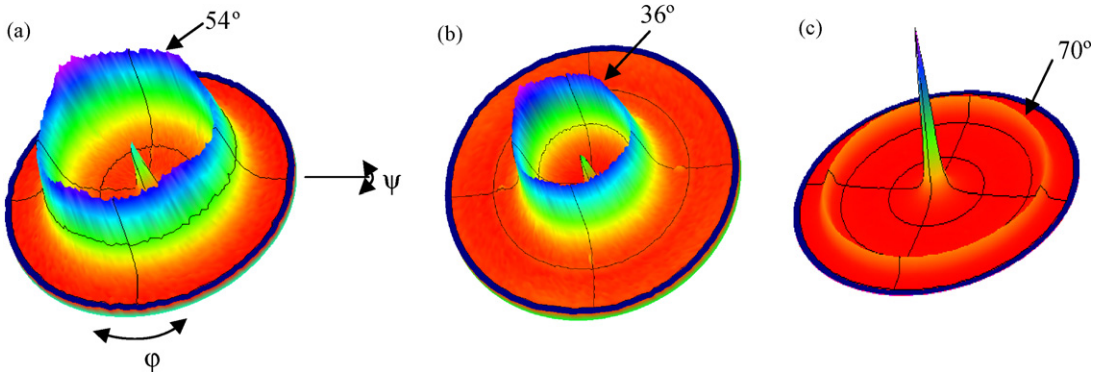

Fig. 4. Phi scan spectra taken about the (a) (1 0 0), (b) (1 1 0) and (c) (1 1 1) peaks, respectively.

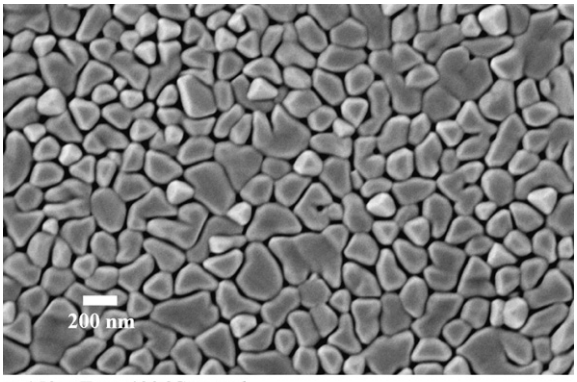

a. 150 mTorr, 400 °C anneal

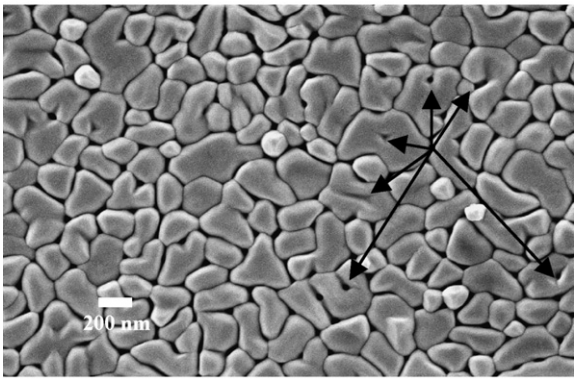

b. 150 mTorr, 600 °C anneal

Fig. 5. SEM images of films deposited at 150 mTorr and annealed at (a) 400 °C and (b) 600 °C.

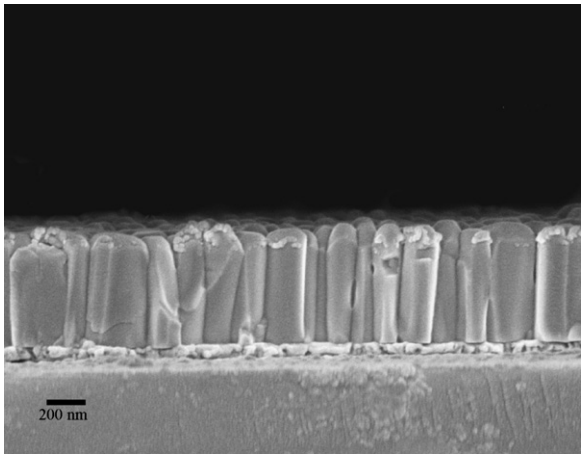

Fig. 6. Cross-section SEM image of a fractured surface, showing dense columnar grain growth.

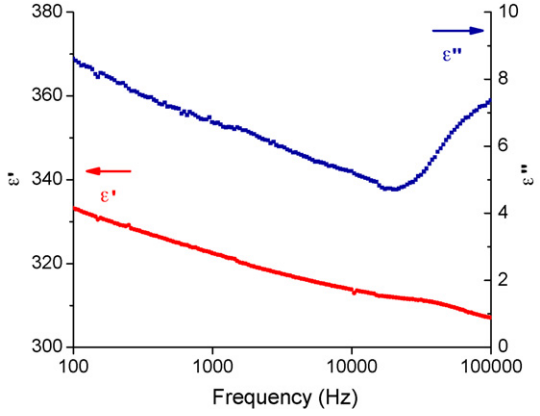

Fig. 7. Variation of permittivity and dielectric loss with frequency at 20 °C.

dielectric relaxation above 100 kHz, whilst the gradual increase in both the real and imaginary parts with decreasing frequency is suggestive of a significant contribution from conductivity. The value of permittivity is substantially higher than the values reported elsewhere (200[27] and 160[24] for sputter deposition; 177 for 350 nm thick electrostatic spray deposition[28]; 210 for 750 nm thick films deposited by spray pyrolysis[29]). However, the value compares well with permittivity data reported by Kigelman et al.[30]

Impedance spectroscopy of the film was carried out at elevated temperature. Fig. 8a shows a complex plane impedance plot, while Fig. 8b shows a comparison of the Z″ and M″ spectroscopic plots at 267 °C, for the film deposited under 150 mTorr of oxygen and annealed at 600 °C. The data was fitted using the ZView software (Scribner Associates Inc, Southern Pines, U.S.A). It exhibits a resistivity of 1710 Ω m and a permittivity of 445 at 267 °C. The coincident Z″ and M″ peaks are indicative of a single RC element.[31]

Fig. 9 is an Arrhenius plot of high temperature resistivity extracted from the impedance data. The film exhibits an activation energy of 1.2 eV. A room temperature resistivity of $\sim 5 \times 10^{11}$ Ω m for the film annealed at 600 °C, was estimated by extrapolating the Arrhenius plot in Fig. 9. Pignolet et al. have also reported a room temperature resistivity of the order of $\sim 10^{11}$ Ω m for sputtered lead titanate films.[27]

The d.c. leakage current behaviour was measured at 85 °C. Fig. 10 is a plot of ln(J) versus ln(E) and shows four distinct

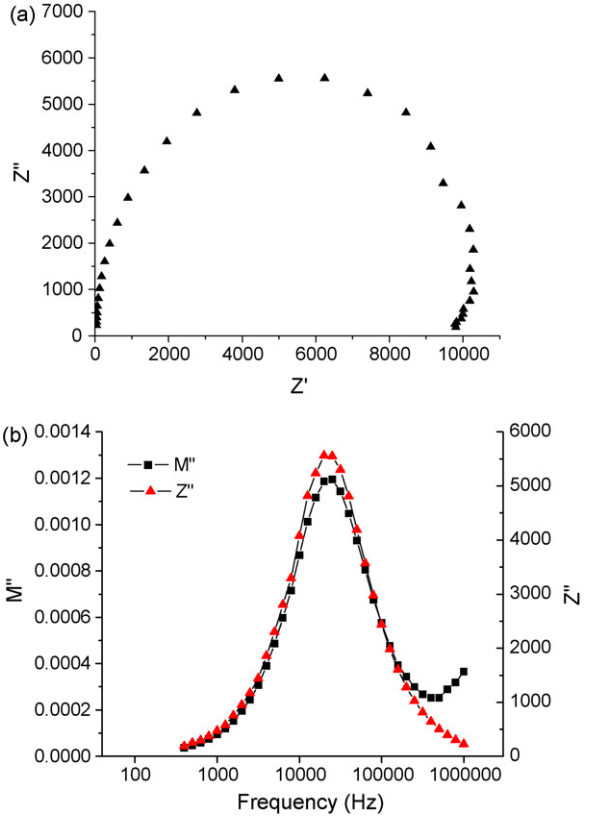

Fig. 8. (a) Complex plane plot of impedance. (b) Comparison of the Z″ and M″ spectroscopic plots at 267 °C.

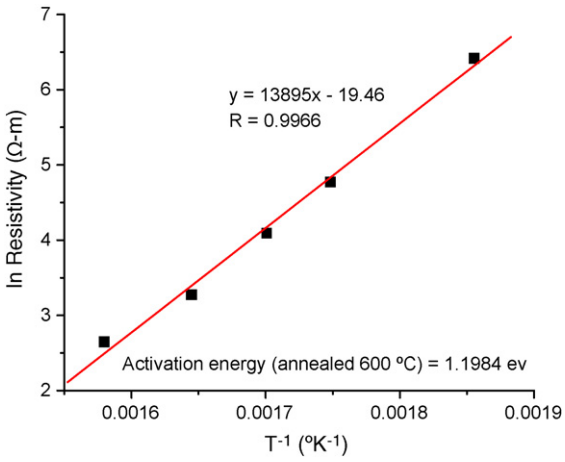

Fig. 9. Arrhenius plot of resistivity for films deposited under 150 mTorr of oxygen and annealed at 600 °C.

regions of varying slopes, defined by the nonlinearity coefficient α.[32] In general the leakage characteristics of the films, exhibit trap influenced space charge limited current (SCLC) behaviour. In the low field region (section A) α has a value of 1.16, corresponding to ohmic behaviour. In region B (13–24 kV/cm) we see an increase in the conductivity of the films, with α increasing to a value of ∼4, corresponding to the shallow trap filling square law. In region C, α reaches a maximum value of 10.62 and appears to be the region of trap filled limit, followed by region D ($\alpha \approx 5$) where all the traps are filled and the trap-free square law is applicable.

For fields of around 12 kV/cm, at the upper limit of ohmic behaviour, the resistivity is only 10^9 Ω m, two orders of magnitude less than that predicted by high temperature measurements. This suggests that there are two conduction mechanisms present: a low activation energy process, dominant at low temperatures, giving way to a higher activation energy process at high temperatures.

P–E hysteresis loops were obtained with the frequency being varied from 1 kHz to 50 kHz. The effect of the leakage current is substantial below a frequency of 10 kHz. A *P–E* loop

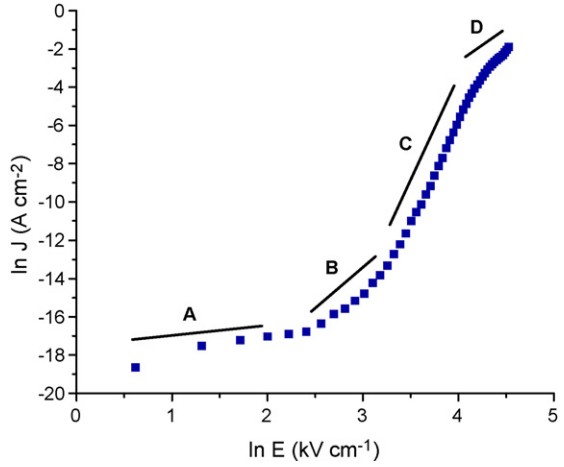

Fig. 10. Plot of ln J vs. ln E showing SCLC behaviour at 85 °C.

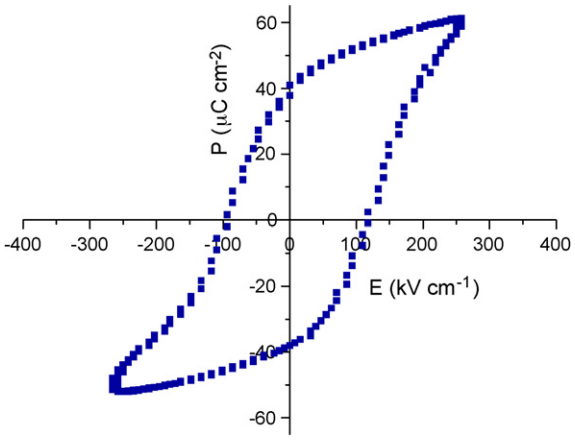

Fig. 11. *P–E* hysteresis loop of a film at 50 kHz, exhibiting a $P_r = 40\ \mu C/cm^2$ and $E_c = 105$ kV/cm.

obtained at an applied field of 270 kV/cm and 50 kHz is shown in Fig. 11. The remanent polarization P_r and coercive field E_c were 40 μC/cm^2 and 105 kV/cm, respectively. It may be noted that Morita et al. have reported P_r up to 96.5 μC/cm^2 with a coercive field ~290 kV/cm for highly epitaxial (0 0 1) PTO films grown on a $SrRuO_3/SrTiO_3$ substrate by a hydrothermal process.[33] As $PbTiO_3$ doesn't exhibit the polarization rotation noted in morphotropic phase boundary PZT, we can estimate a value of P_r in the (1 0 0) direction, by a simple projection onto the [0 0 1] axis resulting in $P_r(0\,0\,1) \approx 73\ \mu C/cm^2$, approximately 25% less than Morita's value.

4. Conclusion

Ferroelectric lead titanate ($PbTiO_3$) films were deposited by pulsed laser deposition on Pt/Si substrates at a substrate temperature of 530 °C. An increase in the oxygen deposition pressure from 100 mTorr to 150 mTorr resulted in enhanced (1 1 1) film orientation. A similar effect was observed on increasing the annealing temperature from 400 °C to 600 °C. The d.c. resistivity at room temperature is approximately $10^9\ \Omega$ m in the ohmic region, with two mechanisms contributing to the observed temperature dependence of conductivity. The conductivity contributes to the high value of relative permittivity at room temperature, but this may also be influenced by the in plane stress observed by X-ray diffraction. *P–E* hysteresis loops for 0.5 μm films obtained at 50 kHz with a field amplitude of 270 kV/cm exhibit a P_r of 40 μC/cm^2 and $E_c = 105$ kV/cm.

References

1. Shirane, G., Hoshino, S. and Suzuki, K., X-Ray study of the phase transition in lead titanate. *Phys. Rev.*, 1950, **80**, 1105–1106.
2. Jona, F. and Shirane, G., *Ferroelectric Crystals*. Dover Publications, Inc., New York, 1993.
3. Wu, C. M., Hong, T. J. and Wu, T. B., Effects of (1 0 0)-textured $LaNiO_3$ electrode on the deposition and characteristics of $PbTiO_3$ thin films prepared by rf magnetron sputtering. *J. Mater. Res.*, 1997, **12**, 2158–2164.
4. Swartz, S. L., Seifert, D. A., Noel, G. T. *et al.*, Characterization of MOCVD $PbTiO_3$ thin-films. *Ferroelectrics*, 1989, **93**, 37–43.
5. Oikawa, M. and Toda, K., Preparation of $Pb(Zr,Ti)O_3$ thin-films by an electron-beam evaporation technique. *Appl. Phys. Lett.*, 1976, **29**, 491–492.
6. Kao, M. C., Wang, C. M., Lee, M. S. *et al.*, Characterization of sol–gel-prepared magnesium-modified lead titanate thin films. *Appl. Phys. A: Mater.*, 2004, **78**, 705–709.
7. Kang, Y. M., Bae, S. C., Ku, J. K. *et al.*, Preparation of epitaxial $PbTiO_3$ thin films by pulsed laser deposition. *Thin Solid Films*, 1998, **312**, 40–45.
8. Chopra, S., Sharma, S., Goel, T. C. *et al.*, Effect of annealing temperature on microstructure of chemically deposited calcium modified lead titanate thin films. *Appl. Surf. Sci.*, 2004, **230**, 207–214.
9. Lee, B. W., Cook, L. P., Schenck, P. K. *et al.*, Processing and characterization of compositionally modified $PbTiO_3$ thin films prepared by pulsed laser deposition. *J. Mater. Res.*, 1997, **12**, 509–517.
10. Dong, Z. G., Shen, M. R. and Cao, W. W., Fatigue-free La-modified $PbTiO_3$ thin films prepared by pulsed-laser deposition on $Pt/Ti/SiO_2/Si$ substrates. *Appl. Phys. Lett.*, 2003, **82**, 1449–1451.
11. Vasco, E., Polop, C. and Ocal, C., Growth atomic mechanisms of pulsed laser deposited La modified-$PbTiO_3$ perovskites. *Eur. Phys. J. B*, 2003, **35**, 49–55.
12. Demczyk, B. G., Rai, R. S. and Thomas, G., Ferroelectric domain-structure of lanthanum-modified lead titanate ceramics. *J. Am. Ceram. Soc.*, 1990, **73**, 615–620.
13. Thomas, R. and Dube, D. C., Structural, electrical and optical properties of sol–gel processed lead titanate thin films. *Jpn. J. Appl. Phys. 1*, 1997, **36**, 7337–7343.
14. Lai, Y. C., Lin, J. C. and Lee, C. P., Nucleation and growth of highly oriented lead titanate thin films prepared by a sol–gel method. *Appl. Surf. Sci.*, 1998, **125**, 51–57.
15. Fu, D. S., Ogawa, T., Suzuki, H. *et al.*, Thickness dependence of stress in lead titanate thin films deposited on Pt-coated Si. *Appl. Phys. Lett.*, 2000, **77**, 1532–1534.
16. Roemer, A., Millon, E., Seiler, W. *et al.*, Correlation between structural and mechanical properties of $PbTiO_3$ thin films grown by pulsed-laser deposition. *Appl. Surf. Sci.*, 2006, **252**, 4558–4563.
17. Kim, Y. K., Kim, S. S., Shin, H. *et al.*, Thickness effect of ferroelectric domain switching in epitaxial $PbTiO_3$ thin films on Pt(0 0 1)/MgO(0 0 1). *Appl. Phys. Lett.*, 2004, **84**, 5085–5087.
18. Roemer, A., Essahlaoui, A., Pons-Y-Moll, O. *et al.*, Growth of lead titanate thin film waveguides by pulsed-laser deposition. *Thin Solid Films*, 2004, **453**, 417–421.
19. Roemer, A., Millon, E., Vincent, B. *et al.*, Epitaxial $PbTiO_3$ thin films grown on (1 0 0) MgO by pulsed-laser deposition for optical waveguiding properties. *J. Appl. Phys.*, 2004, **95**, 3041–3047.
20. Wu, Y. M. and Lo, J. T., Growth of $PbTiO_3$ thin film on Si(1 0 0) with Y_2O_3 and CeO_2 buffer layer. *Jpn. J. Appl. Phys. 1*, 1998, **37**, 4943–4948.
21. Wu, Y. M. and Lo, J. T., Dielectric properties of $PbTiO_3$ thin films on $CeO_2/Si(1\,0\,0)$ and $Y_2O_3/Si(1\,0\,0)$. *Jpn. J. Appl. Phys. 1*, 1998, **37**, 5645–5650.
22. Purandare, S. C., Palkar, V. R., John, J. *et al.*, *C*-axis oriented ferroelectric thin films of Si-substituted $PbTiO_3$ on Si(1 0 0) by pulsed laser deposition: boost for nonvolatile memory application. *Appl. Phys. Lett.*, 1998, **72**, 1179–1181.
23. Fu, D. S., Ohno, T., Ogawa, T. *et al.*, Raman studies of the effects of Nb dopant on the ferroelectric properties in lead titanate thin film. *Jpn. J. Appl. Phys. 1*, 2000, **39**, 5687–5690.
24. Jaber, B., Remiens, D., Cattan, E. *et al.*, Characterization of ferroelectric and piezoelectric properties of lead titanate thin films deposited on Si by sputtering. *Sensor Actuators A: Phys.*, 1997, **63**, 91–96.
25. Chen, C. H., Ryder, D. F. and Spurgeon, W. A., Synthesis and microstructure of highly oriented lead titanate thin-films prepared by a sol–gel method. *J. Am. Ceram. Soc.*, 1989, **72**, 1495–1498.
26. Lotgering, F. K., Topotactical reactions with ferrimagnetic oxides having hexagonal crystal structures 1. *J. Inorg. Nucl. Chem.*, 1959, **9**, 113–123.
27. Pignolet, A., Schmid, P. E., Wang, L. *et al.*, Structure and electrical-properties of sputtered lead titanate thin-films. *J. Phys. D Appl. Phys.*, 1991, **24**, 619–621.

28. Huang, H., Yao, X., Wu, X. Q. *et al.*, Morphology control of ferroelectric lead titanate thin films prepared by electrostatic spray deposition. *Thin Solid Films*, 2004, **458**, 71–76.
29. Murugavel, P., Sharma, R., Raju, A. R. *et al.*, A study of ferroelectric thin films deposited on a $LaNiO_3$ barrier electrode by nebulized spray pyrolysis. *J. Phys. D: Appl. Phys.*, 2000, **33**, 906–911.
30. Kighelman, Z., Damjanovic, D., Cantoni, M. *et al.*, Properties of ferroelectric $PbTiO_3$ thin films. *J. Appl. Phys.*, 2002, **91**, 1495–1501.
31. Sinclair, D. C. and West, A. R., Impedance and modulus spectroscopy of semiconducting batio3 showing positive temperature-coefficient of resistance. *J. Appl. Phys.*, 1989, **66**, 3850–3856.
32. Sato, E., Huang, Y. H., Kosec, M. *et al.*, Lead loss, preferred orientation, and the dielectric-properties of sol–gel prepared lead titanate thin-films. *Appl. Phys. Lett.*, 1994, **65**, 2678–2680.
33. Morita, T. and Cho, Y., A hydrothermally deposited epitaxial $PbTiO_3$ thin film on $SrRuO_3$ bottom electrode for the ferroelectric ultra-high density storage medium. *Integr. Ferroelectr.*, 2004, **64**, 247–257.